JOURNAL OF MATERIALS SCIENCE: MATERIALS IN MEDICINE **16** (2005) 129–133

Synthesis and characterization of fluorine-containing hydroxyapatite by a pH-cycling method

H. QU, M. WEI*
Department of Metallurgy and Materials Engineering, University of Connecticut, 97 North Eagleville Road, Box U-136, Storrs, CT 06269-3136, USA
E-mail: m.wei@ims.uconn.edu

Different fluorine-containing hydroxyapatite (FHA) powders were synthesized through a pH-cycling method by varying sodium fluoride (NaF) concentration in hydroxyapatite (HA) suspensions. The powders were then calcined at 1200 °C for 1 h. Both uncalcined and calcined powders were characterized using X-ray diffraction (XRD), Fourier transform infra-red (FTIR), and F-electrode. It was discovered that fluorine incorporation increased with the fluorine content in the initial solution and the number of pH cycles employed. A relatively low fluorine incorporation efficiency, ~60%, was attained for most of the FHA samples, and it did not vary significantly after calcination. It was also revealed that the FHA particles produced by the pH-cycling method were inhomogeneous. They were a mixture of hydroxyapatite and F-rich apatite (or FA) particles. After calcination, however, these FHA particles were homogenized and became single phased FHA.

1. Introduction

Hydroxyapatite (HA), the main inorganic phase of human hard tissue [1], is widely used as implants or repair materials for bones and teeth. Due to its excellent bioactivity but poor mechanical properties as a bulk material [2], it has been mainly used in non-load bearing situations [1] or as a coating on metallic implant substrates, such as titanium and titanium alloys [3]. However, the long-term performance of HA is still questionable [4]. The resorption and degradation of HA may influence the reliability and lifetime of the implants and ultimately lead to their failure.

Fluorine-containing hydroxyapatite (FHA), where F^- partially replaces OH^- in HA, is more stable than HA *in vivo* [5]. Fluorine ions can stimulate extracellular matrix formation *in vitro* and enhance bone union *in vivo* [6–8]. Thus, FHA is a potential candidate for biological applications. However, it was reported that implants made of fluorapatite (FA), where all the OH^- groups in HA were replaced by F^-, were not osteo-conductive due to the high stability of FA [9]. In addition, high F^- concentration in bone might lead to severe adverse effects such as osteomalacia [10]. Therefore, it is necessary to tailor the F^- content in fluorine-substituted hydroxyapatite so as to optimize the bioactivity of the implants.

There are several methods of synthesizing fluoridated hydroxyapatite with varied fluorine contents, such as pH-cycling [11], solid reaction [12], sol-gel [13], and pyrolysis methods [14]. The pH-cycling method was first introduced by Duff [11] to avoid high temperature operation and usage of volatilized alcohol (fluorine containing reagent). By immersing HA powder in a solution containing certain amount of fluorine ions, the fluorine content in HA was increased by repeatedly fluctuating the pH (usually 4–7) of the solution. In our study, FHA with different fluorine levels were prepared by a pH-cycling method, and the resulting FHA powders were characterized by X-ray diffraction (XRD), Fourier transform infrared spectroscopy (FTIR) and fluorine analysis.

2. Methods

2.1. Synthesis of HA and FHA

Synthesizing HA involved a metathesis reaction. 300 ml of 1 M calcium nitrate (99%, Sigma) and 600 ml of 0.3 M diammonia phosphate (99%, Sigma) solutions were prepared, and the pH of each solution was brought up to 11–12 by adding strong ammonia (29.5%, Sigma). The phosphate solution was slowly added to the calcium nitrate solution, resulting in the precipitation of HA. The precipitates were aged for 7 days at room temperature. They were then thoroughly washed with deionized water and dried in an oven at 80 °C for 16 h. Finally, the precipitates were ground into a fine powder using an agate mortar and pestle.

FHA with varied fluorine contents were synthesized as follows: 2 liters of sodium fluoride (100%, Sigma)

*Author to whom all correspondence should be addressed.

TABLE I Materials tested

NaF/HA molar ratio in initial solution	Uncalcined	Calcined at 1200 °C for 1 hr
0	FHA0	Cal-FHA0
0.25	FHA1	Cal-FHA1
0.50	FHA2	Cal-FHA2
0.75	FHA3	Cal-FHA3
1.00	FHA4	Cal-FHA4

solutions with concentrations of 2.5×10^{-3}, 5×10^{-3}, $7.5 \times 10^{-3}$and 1×10^{-2} M, were prepared respectively. 10 g of the HA powder produced above was suspended in each of the sodium fluoride solution in order to prepare 25, 50, 75 and 100% fluorine substituted hydroxyapatite (FHA). The solutions were equilibrated at pH 7 overnight. The pH of the solution was then brought down to 4 by slowly dropping 1 M HNO_3 (70%, Aldrich) to each solution. After 30 min, the pH of each solution was brought up to 7 again by adding 1 M NaOH (1 N standard solution, Acros). The pH cycling process was repeated three times. The precipitates were then aged for one day at room temperature.

After the pH cycling, the precipitates were subsequently washed five times with deionized water to eliminate sodium residues remaining in the solution. They were then dried at 80 °C for 24 h and ground into fine powders. FHA powders at each composition were calcined at 1200 °C for 1 h in air. The sample name and composition are listed in Table I.

2.2. XRD and FTIR analyses

Both uncalcined and calcined HA and FHA powders were examined using X-ray diffractometer (BRUKER AXS D5005) with a copper target. The voltage and current used were 40 kV and 40 mA, respectively. A step size of 0.02° and a scan speed of 1°/min were used for the broad-range XRD. A short-range XRD was also conducted for both uncalcined and calcined HA and FHA powders with the same step-size and a scan speed of 0.05°/min. Further, all the specimens were examined by FTIR (Nicolet Avatar 360) at a resolution of 4 cm^{-1}.

2.3. Fluorine measurement

Fluorine concentration measurement was conducted using F-selective electrode (Orion 94-09) in a total ionic strength adjustment buffer (TISAB). 0.2 g of each sample was dissolved in 10 ml of 1 M nitric acid and then diluted by 200 ml deionized water. The fluorine content was determined by mixing 10 ml of such solution and 10 ml of the buffer. Standard solutions made from NaF were used to calibrate the measurement in the same buffer solution.

3. Results

3.1. X-ray diffraction

Similar broad-range XRD patterns were obtained for all the uncalcined specimens. No other phase than apatite was detected, which suggested that pure apatite was achieved for all the uncalcined specimens. However,

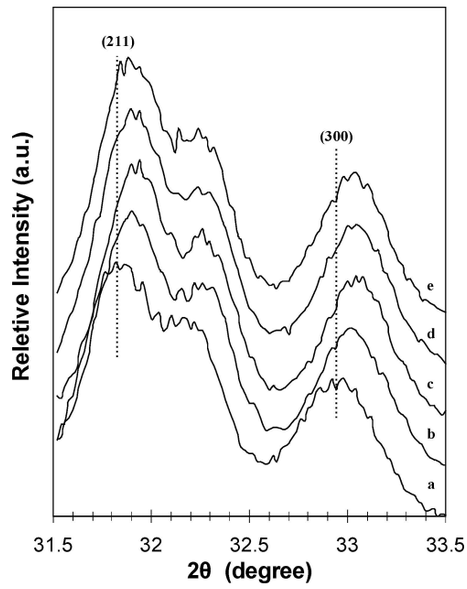

Figure 1 Short-range XRD pattern of (a) FHA0, (b) FHA1, (c) FHA2, (d) FHA3, and (e) FHA4.

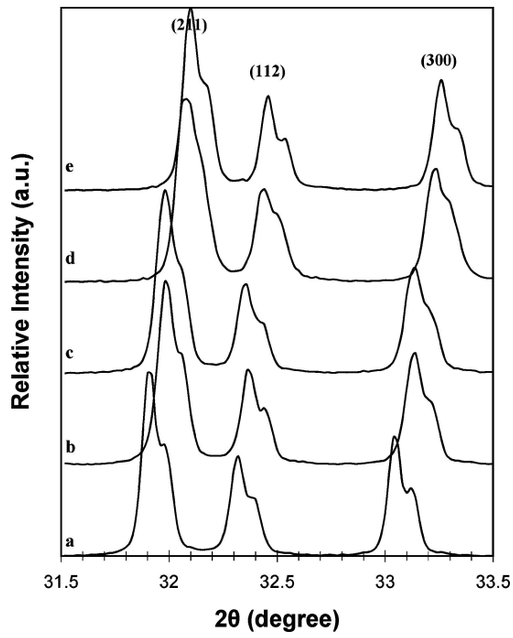

Figure 2 Short-range XRD pattern of (a) Cal-FHA0, (b) Cal-FHA1, (c) Cal-FHA2, (d) Cal-FHA3, and (e) Cal-FHA4.

it was detected by short-range XRD examinations (as shown in Fig. 1) that both 211, 112, and 300 peaks of all the fluorine-containing samples shifted to a higher angle comparing to FHA0 (pure HA), but no difference was seen among these samples. After calcination, however, the shift of the 211, 112 and 300 peaks of the fluorine containing specimens to higher angles varied systematically with increasing fluorine content (Fig. 2). Nevertheless, broad-range XRD data revealed that phase pure apatite was obtained for all the samples including FHA0 (pure HA) after calcining at 1200 °C for 1 h (Fig. 3). Tricalcium phosphate (TCP) was not detected by XRD in any of these samples.

TABLE II Fluorine concentration of uncalcined and calcined samples

Sample (uncalcined)	Fluorine ion contend (mol F/mol Apatite)	Sample (calcined at 1200°C)	Fluorine ion contend (mol F/mol Apatite)
FHA1	0.232 ± 0.012	Cal-FHA1	0.224 ± 0.035
FHA2	0.314 ± 0.034	Cal-FHA2	0.321 ± 0.017
FHA3	0.425 ± 0.034	Cal-FHA3	0.415 ± 0.022
FHA4	0.569 ± 0.062	Cal-FHA4	0.557 ± 0.037

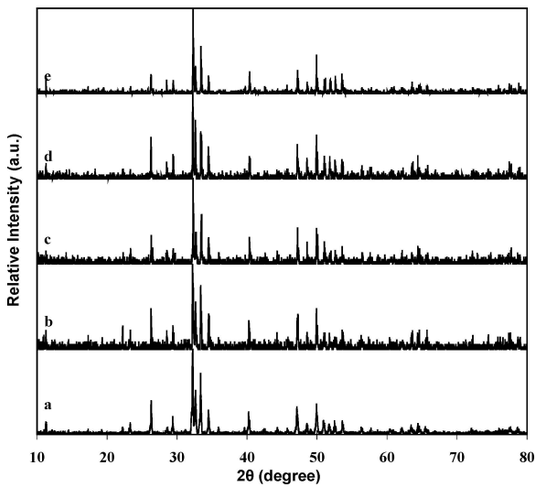

Figure 3 Broad-range XRD pattern of (a) Cal-FHA0, (b) Cal-FHA1, (c) Cal-FHA2, (d) Cal-FHA3, and (e) Cal-FHA4.

3.2. Fluorine analyses

Table II lists the fluorine concentration of all the specimens before and after calcination. After calcination, the fluorine content in the calcined specimens was slightly varied from their corresponding uncalined forms, but the difference was less than 10% in all the cases. The fluorine concentrations in both uncalcined and calcined specimens increased with the fluorine content added to the initial solution during the powder synthesis, but they were significantly lower than those added to the initial solutions except for the specimens FHA1 and Cal-FHA1. A fluorine incorporation efficiency, ∼60%, was attained for most of the FHA samples.

To study the fluorine incorporation, the F^-content in both FHA4 precipitates and the remaining solutions at each pH cycle was measured (Table III). It demonstrated that with the increase of the fluorine content in the precipitates, the fluorine concentration in the solution decreased. At cycle 0, no fluorine was incorporated into HA. As a result, the fluorine content in the precipitates was 0, and that in the solution was 1.00×10^{-2} mol/l, which was the initial fluorine content added to the solution. After the first pH cycling, about 40% (0.421 mol fluorine in 1 mol HA) of the fluorine had incorporated into the HA structure. Completing all the three cycles, about 50% (0.551 mol fluorine in 1 mol HA) of the fluorine ions had incorporated into HA structure, and the rest was left in the solution, which was removed in the subsequent washing process.

TABLE III The fluorine concentration of both the precipitates and corresponding solutions at each pH cycle of FHA4

	Fluorine contend of precipitations (mol F/mol Apatite)	Fluorine contend of solution (mol/L)
Cycle 0	0	1.00×10^{-2}
Cycle 1	0.421	6.24×10^{-3}
Cycle 2	0.526	5.00×10^{-3}
Cycle 3	0.551	5.01×10^{-3}

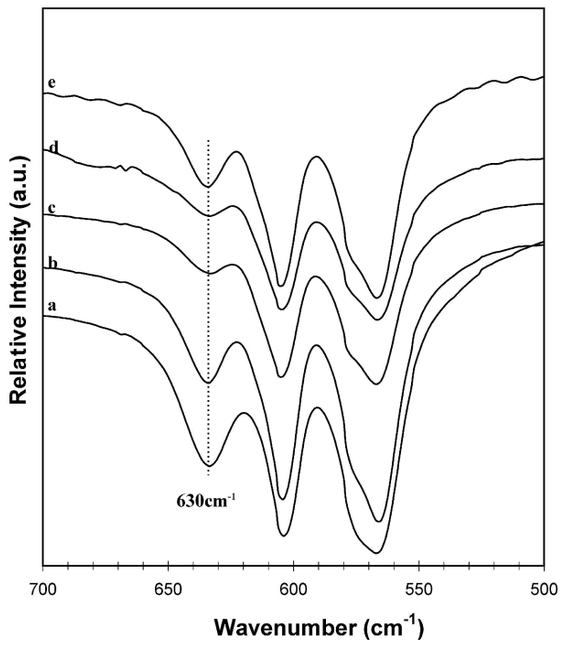

Figure 4 FTIR spectra of (a) FHA0, (b) FHA1, (c) FHA2, (d) FHA3, and (e) FHA4 at lower wavenumbers.

3.3. FTIR analysis

The FTIR data (Figs. 4 and 5) of both the uncalcined HA and FHA samples showed that with an increase in sodium fluoride content in the initial solution, the intensity of both OH^- librational band at 630 cm^{-1} and OH^- stretching band at 3571 cm^{-1} became weak, but these bands were still observable in all five uncalcined specimens. In comparison, after calcination, except for pure hydroxyapatite (Cal-FHA0), both 630 $cm^{-1}$and 3571 cm^{-1} peaks disappeared in all the fluorine containing specimens (i.e., Cal-FHA1, Cal-FHA2, Cal-FHA3, and Cal-FHA4), but a new 3545 cm^{-1} peak was appeared in Cal-FHA2, Cal-FHA3 and Cal-FHA4 samples which was due to the vibration of the F-OH band (Figs. 6 and 7).

4. Discussion

During the pH drop from 7 to 4, the Ca^{2+} ions dissociates from the surface of hydroxyapatite particles [15]. Because of their strong tendency to react with F^- [12],

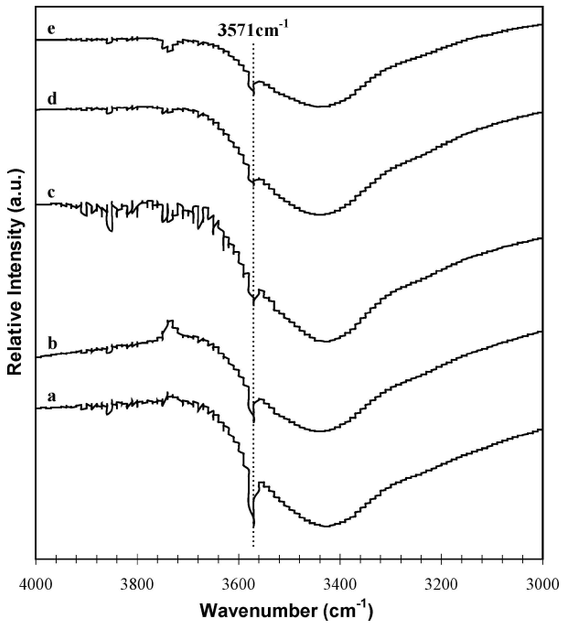

Figure 5 FTIR spectra of (a) FHA0, (b) FHA1, (c) FHA2, (d) FHA3, and (e) FHA4 at high wavenumbers.

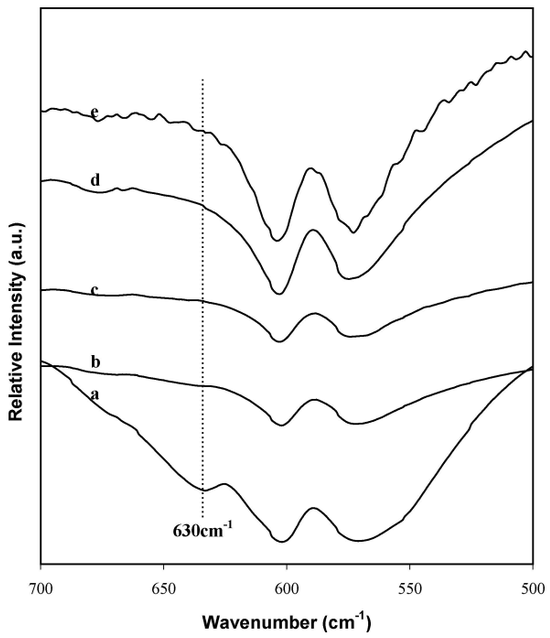

Figure 6 FTIR spectra of (a) Cal-FHA0, (b) Cal-FHA1, (c) Cal-FHA2, (d) Cal-FHA3, and (e) Cal-FHA4 at lower wavenumbers.

Ca^{2+} ions rapidly consumes F^- ions in the solution to form CaF_2. When pH is raised to 7, the newly formed CaF_2 fine particles further react with HPO_4^{2-} or $H_2PO_4^-$ in the solution to form fluoridated-hydroxyapatite precipitations [16]. The reaction can be expressed as below:

$$\begin{aligned} &Ca_5(PO_4)_3OH + 10F^- + (7-m)H^+ \\ &\longrightarrow 5CaF_2 + H_2O + (3-m)H_2PO_4^- + mHPO_4^{2-} \end{aligned} \tag{1}$$

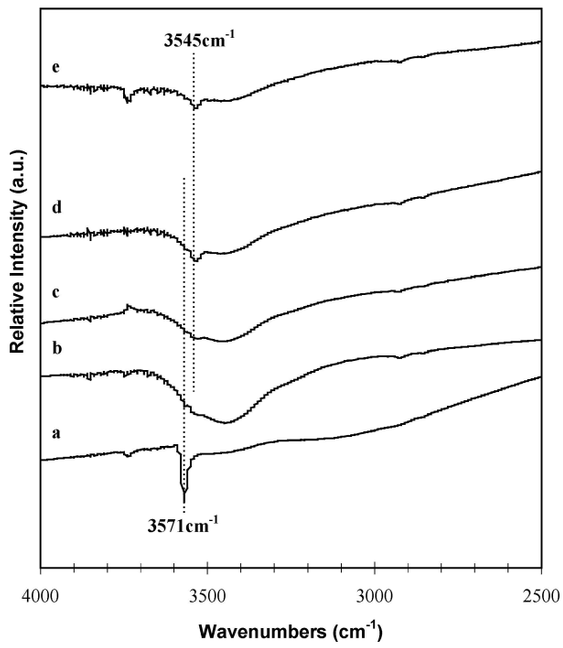

Figure 7 FTIR spectra of (a) Cal-FHA0, (b) Cal-FHA1, (c) Cal-FHA2, (d) Cal- FHA3, and (e) Cal-FHA4 at higher wavenumbers.

$$\begin{aligned} &5CaF_2 + (3-m)H_2PO_4^- + mHPO_4^{2-} + (1-x)H_2O \\ &\longrightarrow Ca_5(PO_4)_3(OH)_{1-x}F_x + (10-x)F^- \\ &\quad + (7-x-m)H^- \quad (0<x<1, 0<m<3) \end{aligned} \tag{2}$$

Combining Eqs. (1) and (2), the chemical reaction at each pH cycle can be written as:

$$\begin{aligned} &Ca_5(PO_4)_3(OH) + xF^- + xH^+ \\ &\longrightarrow Ca_5(PO_4)_3F_x(OH)_{1-x} + xH_2O \end{aligned} \tag{3}$$

At the second pH-cycle, more F^- incorporates into HA. Like the first pH-cycle, more F^- reacts with the dissociated Ca^{2+} from HA surfaces and forms F-rich apatite or FA. Similar chemical reactions also occur in the third pH-cycle. It is evident from Table II that the more fluorine added to the initial solution, the higher the fluorine content in the precipitates, and the lower the F^- concentration in the remaining solution. With the increase of the pH cycles, the fluorine content in the remaining solution decreased (Table III). However, the rate of F^- incorporation at each pH cycle was different. Taking FHA4 as an example, approximately 40% of the fluorine in the solution had incorporated into HA after the first pH cycle, but only extra 10% fluorine was incorporated after the second cycle, and almost no F^- incorporation occurred in the third cycle (Table III). On average, the total fluorine incorporation in all the fluorine containing samples after three pH cycles was about 60% (except for FHA1), and 40% of the fluorine added to the solution remained unreacted. Calcination did not enhance the rate of fluorine incorporation (Table II). Duff [11] also reported that excessive F^- was required to achieve completely fluorine-substituted apatite, $Ca_5(PO_4)_3F$.

At each pH cycle, some HA particles had reacted with F^- in the solution and formed F-rich apatite or FA, while the rest of HA remained un-reacted. As a result, identical XRD patterns were observed for specimens FHA1, FHA2, FHA3, and FHA4, as these samples were a mixture of HA and F-rich apatite (or FA) at different ratios. However, they were substantially different from FHA0 (pure HA) that was absent of fluorine ions. Furthermore, the FTIR spectra (Figs. 4 and 5) of all the precipitates demonstrated that two bands at 631 cm^{-1} and 3571 cm^{-1} attributed to OH^- were observed in all these specimens, which was due to the presence of HA in all the precipitates. It was also observed that the higher the fluorine content in the precipitates, the lower the intensity of the OH^- bands. As a result, all the fluorine containing uncalcined specimens were a mixture of HA and F-rich apatite (or FA). With the increase of the fluorine content in the initial solution, the HA content in the precipitates decreased while F-rich apatite (or FA) increased.

During the calcination process, the F^--rich apatite (FA) and HA turned into a homogenous, single-phased FHA (Fig. 3), where the 300 peak of all the calcined samples shifted to a higher angle with the increase of fluorine content (Fig. 2). It was reported by Okazaki *et al.* [14] that with the increase of fluorine content, the *a*-axis parameter decreased and the unit cell of apatite shrank resulting in the 300 peak shifting to a higher angle, which suggested that more fluorine had replaced the OH^- groups in the apatite. Also, the FTIR spectra (Figs. 6 and 7) demonstrated that both 630 cm^{-1} and 3571 cm^{-1} vibrations disappeared in all the fluorine-containing calcined specimens. Freund and Knobel [17] revealed that the intensity of both OH^- vibration band at 630 cm^{-1} and OH^- stretching band at 3571 cm^{-1} decreased when F^- was incorporated into the HA lattice. If more than 30% of the F^- was incorporated into the HA lattice, a new band appeared at 3543 cm^{-1} vibration [18], which was observed in the three high F^- containing samples, Cal-FHA2, Cal-FHA3 and Cal-FHA4 (Fig. 7).

5. Conclusions

FHA with varied fluorine contents were synthesized through a pH cycling method. The results indicated that less than 60% of the initial fluorine was incorporated into the OH^- position in the apatite structure for most of the FHA samples. It was also concluded that the initial precipitate was a mixture of HA and F-rich apatite (or FA). After calcination, the mixture was converted into homogenous fluoridated hydroxyapatite.

Acknowledgments

The authors would like to thank Prof. Pedro Cid-Aguero for his assistance with fluorine analysis.

References

1. E. SHORS and R. HOLMES, in An Introduction to Bioceramics, edited by L. L. Hench and J. Wilson (World Scientific, Singapore, 1993) p. 181.
2. J. PARK and R. LAKES, in "Biomaterials: An Introduction" (Plenum Press, New York, 1992) p. 193.
3. W. WENG, S. ZHANG, K. CHENG, H. QU, P. DU, G. SHEN, J. YUAN and G. HAN, *Surface and Coatings Tech.* **167** (2003) 292.
4. S. OVERGAARD, M. LIND, K. JOSEPHSEN, A. MAUNSBACH, C. BÜNGER and K. SOBALLE, *J. Biom. Mater. Res.* **39** (1998) 141.
5. M. OKAZAKI, Y. MIAKE, H. TOHDA, T. YANAGISAWA, T. MATSUMOTO and J. TAKAHASHI, *Biomaterials* **20** (1999) 1421.
6. M. SUNDFELDT, M. WIDMARK, A. WENNERBERG, J. KÄRRHOLM, C. JOHANSSON and L. CARLSSON, *J. Mater. Sci. Mater. Med.* **13** (2002) 1037.
7. S. MIKAEL, P. JAN, S. JANOS, W. ANN, K. JOHAN, B. CARINA and V. LARS, *ibid.* **13** (2002) 1045.
8. K. LAU, C. GOODWIN, M. ARIAS, S. MOHAN and D. BAYLINK, *Bone* **30** (2002) 705.
9. E. LUGSCHEIDER, M. KNEPPER, B. HEIMBERG, A. DEKKER and C. KIRKPATRICK, *J. Mater. Sci. Mater. Med.* **5** (1994) 371.
10. K. W. LAU, K. ÅKESSON, C. R. LIBANATI and D. J. BAYLINK, in Anabolic Treatments for Osteoporosis, edited by J. F. Whitfield and P. Morley (CRC Press, Boca Raton, 1998) p. 207.
11. E. J. DUFF, *Caries. Res.* **7** (1973) 231.
12. G. FISCHMAN, A. CLARE and L. HENCH, in Ceramic Transactions, Bioceramics: Materials and Applications (American Ceramic Society, Westerville, OH, 1995) Vol. 48, p. 283.
13. K. CHENG, G. HAN, W. WENG, H. QU, P. DU, G. SHEN, J. YANG and J. F. FERREIRA, *Mater. Res. Bull.* **38** (2003) 89.
14. U. PARTENFELDER, A. ENGEL, and C. RUSSEL, *J. Mater. Sci. Mater. Med.* **4** (1993) 292.
15. W. E. BROWN and L. C. CHOW, *J. Crystal Growth* **53** (1981) 31.
16. L. M. RODRIGUEZ-LORENZO and K. A. GROSS, *Bioceramics* **15** (2003) 587.
17. F. FREUND and R. M. KNOBEL, *J C S Dalton Trans* **11** (1977) 1136.
18. A. BAUMER, M. GANTEAUME and W. E. KLEE, *Bull. Mineral.* **108** (1985) 145.

Received 8 January
and accepted 20 July 2004